

Optical Engineering

OpticalEngineering.SPIEDigitalLibrary.org

Modeling of the laser beam shape for high-power applications

Jan K. Jabczyński
Mateusz Kaskow
Lukasz Gorajek
Krzysztof Kopczyński
Waldemar Zendzian

SPIE.

Jan K. Jabczyński, Mateusz Kaskow, Lukasz Gorajek, Krzysztof Kopczyński, Waldemar Zendzian, "Modeling of the laser beam shape for high-power applications," *Opt. Eng.* **57**(4), 046107 (2018), doi: 10.1117/1.OE.57.4.046107.

Modeling of the laser beam shape for high-power applications

Jan K. Jabczyński,* Mateusz Kaskow, Lukasz Gorajek, Krzysztof Kopczyński, and Waldemar Zendzian
Military University of Technology, Institute of Optoelectronics, Warsaw, Poland

Abstract. Aperture losses and thermo-optic effects (TOE) inside optics as well as the effective beam width in far field should be taken into account in the analysis of the most appropriate laser beam profile for high-power applications. We have theoretically analyzed such a problem for a group of super-Gaussian beams taking first only diffraction limitations. Furthermore, we have investigated TOE on far-field parameters of such beams to determine the influence of absorption in optical elements on beam quality degradation. The best compromise gives the super-Gaussian profile of index $p = 5$, for which beam quality does not decrease noticeably and the thermo-optic higher order aberrations are compensated. The simplified formulas were derived for beam quality metrics (parameter M^2 and Strehl ratio), which enable estimation of the influence of heat deposited in optics on degradation of beam quality. The method of dynamic compensation of such effect was proposed. © The Authors. Published by SPIE under a Creative Commons Attribution 3.0 Unported License. Distribution or reproduction of this work in whole or in part requires full attribution of the original publication, including its DOI. [DOI: [10.1117/1.OE.57.4.046107](https://doi.org/10.1117/1.OE.57.4.046107)]

Keywords: laser and laser optics; laser beam shaping; thermal effects.

Paper 171949P received Dec. 6, 2017; accepted for publication Mar. 21, 2018; published online Apr. 13, 2018.

1 Introduction

One of the specific tasks of laser engineering is the transformation of high-power laser beam satisfying special requirements on beam waist size in far field and additionally the restrictions on beam forming optics (sizes, aperture losses, thermal effects, etc.). From the practical point of view, the main limitations in near-field (i.e., inside optics) are posed by thermal effects especially for multi kWatt, complex, multielement optical systems. The “rule of thumb” in engineering practice is that optics should have aperture of about 2 times larger than the laser beam diameter defined for Gaussian profile at $1/e^2$ level, which is not a good choice for mitigation of thermal effects by the way. Thus, the question on the optimal laser beam profile which mitigates thermal effects in near-field optics not degrading brightness and beam width in far field is still open. Let us note that the laser beam quality has to be determined according to $D_{86.5}$ definitions (see Ref. 1), Strehl ratio and second moment definitions are not appropriate measures for such a case. Therefore, beam parameter product (BPP) = $\pi w_{86.5} \theta_{86.5} / \lambda$ defined on the basis of $D_{86.5}$ will be used here as a metrics.

To determine the best laser beam profile, the minimization of aperture losses and thermo-optic effects (TOEs) in near-field as well as the minimal effective width of laser beam in far field should be taken into account. Let us notice that the best from the thermo-optic limitations “top-hat” profile results in far field in multilobe, “sombbrero”-like shape, which has wider $D_{86.5}$ diameter than equivalent Gaussian one. On the other hand, for Gaussian profile of given $1/e^2$ diameter in the near-field, the clear aperture should be wider (~ 2 times), which significantly increases TOEs. Thus, it is an evident trade-off between the above

requirements in near and far fields. Moreover, we have to take into account the manufacturability of beam shaper destined to transform Gaussian beam to the most appropriate shape.

To start the analysis, we have to choose the appropriate basis of beam profiles (see Refs. 2–5). The most convenient for our purposes seems to be the super-Gaussian beams (SGB)^{2,3} and flattened Gaussian beams (FGB).^{4,5} In both cases, the analytical method for M^2 parameter calculations was found,^{3,4} whereas for BPP calculations the numerical approach is required. Both approaches (SGB and FGB) should lead to the same results in principle.⁵ We have taken for our purposes the SGBs because of the simpler mathematical description important for numerical simulations and wide diversity of shapes especially for close to Gaussians profiles. Moreover, the technical realization of diffraction limited beam shapers transforming Gaussian beam into SGB is well known (see e.g., Refs. 6 and 7).

In Sec. 2, we have analyzed such a problem for SGBs taking only diffraction effects into account. In Sec. 3, we have analyzed TOEs for such cases. The typical laser system consists of several elements, including mirrors and refractive elements, and each experiences the TOEs as a result of residual absorption on surfaces and in the volume. We have modeled the influence of TOEs on the far-field parameters of SGB beams applying COMSOL software⁸ for two cases: volume heat density source and surface heat source for idealized heat contacts. The results of numerical analysis undertaken for given heat power can be rescaled to other cases applying the simple relations given at the end of paper.

2 Diffraction Analysis for Super-Gaussian Beams

To analyze the parameters of the laser beam of a different profile in far field, we have chosen a family of SGB defined in near-field as follows:

*Address all correspondence to: Jan K. Jabczyński, E-mail: jan.jabczynski@wat.edu.pl

$$SG_p(x, w_p) = N_p(w_p)^{-1/2} \exp[-(x/w_p)^2 p], \quad (1)$$

where SG_p is the amplitude function of SGB of index p , $N_p(w_p) = \pi w_p^2 \Gamma(1/p) 2^{-1/p} p^{-1}$ norm of SG_p accomplishing the unit power of each beam, $\Gamma(x)$ is the gamma function, and w_p is the radius of beam.

Furthermore, we calculated the amplitude functions $SG_{ff,p}$ in far field applying Hankel transform valid for cylindrical symmetry (see details in Ref. 6) as follows:

$$SG_{ff,p}(r_{ff}) = c_p \int_0^{r_{ff, \max}} J_0\left(\frac{kr_{ff}\rho}{f}\right) SG_p(\rho, w_p) \rho d\rho, \quad (2)$$

where c_p is the constant and f is the focal length.

The intensity profiles in near-field for $p = 1, 2, 5$, and 32 are shown in Fig. 1 and corresponding intensity distributions in far field are shown in Fig. 2. For each SG_p , the different beam radii w_p were taken in such a way that it contains 99.95% of SG_p power in the same aperture $D_{\text{aper}} = 2W_{\text{aper}}$ (which corresponds to $W_{\text{aper}} = 2w_1$ for Gaussian beam $p = 1$).

To define beam diameter in far field, power in bucket (PIB) distributions (see Ref. 1) were calculated as follows:

$$\text{PIB}(r_{ff}, p) = \int_0^{r_{ff}} I_{ff,p}(\rho) \rho d\rho / \int_0^{r_{ff, \max}} I_{ff,p}(\rho) \rho d\rho, \quad (3)$$

where $I_{ff,p}(r_{ff}) = |SG_{ff,p}(r_{ff})|^2$ is the intensity profile of SG_p in far field and $r_{ff, \max}$ is the radius in far field, beyond which the intensity is negligible for all p (see Figs. 2 and 3). Knowing PIB distributions, we have determined the beam radius $R_{ff,86.5,p}$ according to criterion of 86.5% of PIB.

Let us notice (see Fig. 1) that for $p = 1$, we have Gaussian beam, whereas for $p = 32$ we have nearly top-hat profile. The criterion of 86.5% of PIB, frequently used in laser engineering (see e.g., Refs. 1, 9, and 10), corresponds to classical $1/e^2$ diameter definition of Gaussian beam. Strictly according to that criterion SG_{32} is better, but it has multilobe shape with wide pedestals in far field (see Figs. 2 and 3); moreover, technical realization of cost-effective beam shapers for such profile is problematic. Applying higher level of criterion, e.g., 95%, the lowest diameter has the SG_5 beam and similar

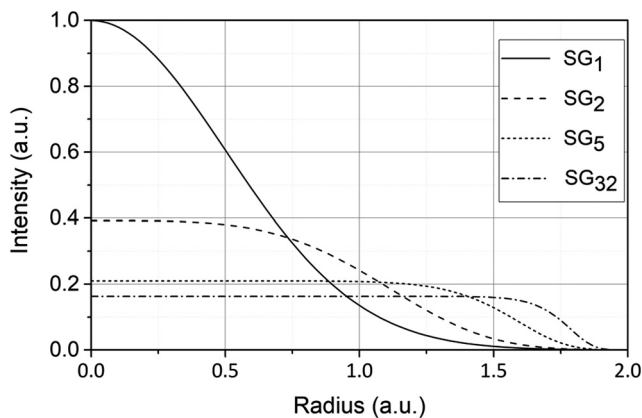


Fig. 1 Intensity versus radius of SG_1 , SG_2 , SG_5 , and SG_{32} beams in near-field having the same aperture losses of 0.05% at radius = 2.

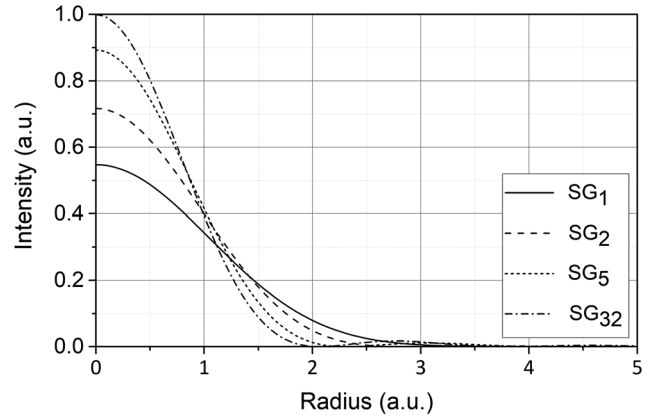


Fig. 2 Intensity distributions of SG_1 , SG_2 , SG_5 , and SG_{32} beams in far field.

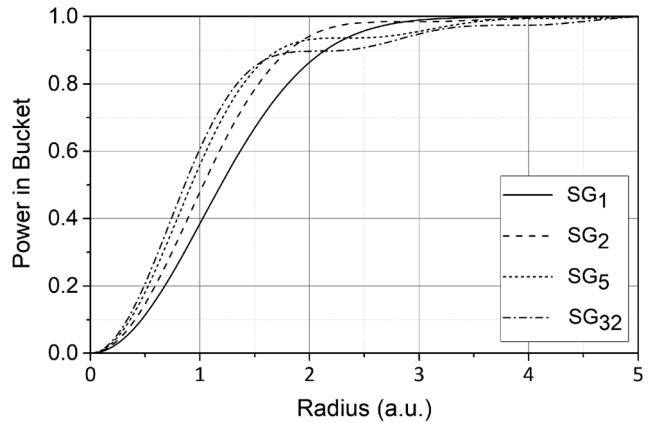


Fig. 3 PIB functions for intensity distributions of SG_1 , SG_2 , SG_5 , and SG_{32} beams in far field.

smooth profile in far field as Gaussian with <5% in pedestal (see Fig. 3).

We can now determine the optical measures being the merit functions in analysis: relative brightness B_p , effective beam parameter product BPP_p , and Strehl ratio SR_p as follows:

$$B_p = A_{nf,1} A_{ff,1} / A_{nf,p} A_{ff,p}, \quad (4)$$

$$BPP_p = \sqrt{B_1 / B_p}, \quad (5)$$

$$SR_p = I_{ff,p}(0) / I_{f,p \max}(0), \quad (6)$$

where $A_{nf,p} = \pi R_{nf,86.5,p}^2$ and $A_{ff,p} = \pi R_{ff,86.5,p}^2$ are the areas of SG_p beam in near and far field, respectively, $R_{nf,86.5,p}$ and $R_{ff,86.5,p}$ are the beam radii of SG_p beam in near and far field determined according to 86.5% criterion, respectively.

To assess the flatness of SG_p profile in near-field, we have introduced additional merit function $MF_{nf,p}$ as a ratio of maximal intensity of SG_1 and SG_p as follows:

$$MF_{nf,p} = |SG_1(0, w_1) / SG_p(0, w_p)|^2. \quad (7)$$

Table 1 Results of calculations of merit functions for $p = 1, 2, 5,$ and 32 .

	$p = 1$	$p = 2$	$p = 5$	$p = 32$
$MF_{nf,p}$	1.000	2.55	4.77	6.75
B_p	1.000	0.85	0.63	0.569
BPP_p	1.000	1.085	1.259	1.326
SR_p	0.576	0.758	0.945	1.000

It is easy to show that for perfect top-hat beam ($p \rightarrow \infty$) $MF_{nf,\infty} = 8$. In Table 1, the results of calculations for a few SG_p beams were collected.

Let us notice that taking into account only the maximum of brightness (or equivalent minimum of BPP), the best is Gaussian beam ($p = 1$) evidently. For the almost top-hat ($p = 32$) beam of equivalent aperture, 43% drop in brightness and 33% increase in BPP were found. However, if we additionally have to consider the profile flatness in near-field, which affects temperature profile and thermally induced distortions, the answer becomes more complicated. Taking both near- and far-field requirements, the best compromise seems to be SG_5 ($p = 5$) beam (blue curves in Figs. 1–3), which has smooth profile in far field, slightly increased BPP ($BPP_5 = 1.259$), but much more flattened profile in near-field ($MF_{nf,5} = 4.77$). Moreover, as we will show in Sec. 3, such profile enables nearly compensation of higher order TOEs.

3 Modeling of Thermal Optics Effects for SG Beams

To investigate the influence of TOEs on beam quality, we have taken the typical optical element of 50-mm diameter, 10-mm thickness made of fused silica. The “idealized” heat contacts (constant temperature on side, and negligible heat transfer to rear and front facet) were assumed. The eight different heat sources (for each SG_p , pair of volume or surface source) were considered.

To compare the effects of such eight different heat sources, we have assumed that the same heat power of 1 W (corresponding to 10-ppm heat conversion for incident 100 kW of laser power) was deposited in optical element. Let us notice that in the best quality fused silica glass, the absorption coefficient is much lower than 10^{-5} 1/cm.^{11–13} The surface absorption is determined by quality of surface itself and the absorption in dielectric coatings. It is possible to achieve the same level of absorption losses in the highest quality mirrors.^{11–13} However, as a result of technical imperfections and superposition of different factors, the realistic value of absorption is estimated of a few dozens of ppm.

For each case, the problem was solved applying COMSOL software,⁸ and three-dimensional (3-D) maps of temperature increase were calculated [see examples for SG_1 and SG_{32} beams in Figs. 4(a)–4(d)].

Next, we calculated the profile of averaged temperature $\Delta T_{avg,i}$ versus radius r_i integrating temperature profile over z -depth. Then, multiplying by effective thermal dispersion coefficient χ_T and b —thickness of sample, the thermally induced optical path difference (OPD) was determined

$$OPD(r, P) \cong \chi_T \cdot \Delta T_{avg}(r, P) \frac{b}{\lambda}, \quad (8)$$

where the effective thermal dispersion for transmission is defined as

$$\chi_T = \frac{dn}{dT} + (1 + \nu_{\text{Poisson}})\alpha_T(n - 1) + \dots \quad (9)$$

The OPD can be divided into paraxial component OPD_{par} and residual nonparaxial OPD_{np} according to the following equation:

$$\begin{aligned} OPD(r, P) &= OPD_{\text{par}}(r, P) + OPD_{\text{np}}(r, P) \\ &= M_T(P) \frac{r^2}{2\lambda} + OPD_{\text{np}}(r, P), \end{aligned} \quad (10)$$

where M_T is the paraxial thermal optical power.

To determine OPD dependence on radius, the mean square approximation of data array $(r_i, \Delta T_{avg,i})$ calculated in COMSOL was applied as follows:

$$\Delta T_{\text{aprox}} = \sum_{m=1}^N a_m r^{2m}. \quad (11)$$

After a few simple transformations

$$M_T = 2 \cdot \chi_T b \cdot a_1, \quad (12)$$

where a_1 is the quadratic coefficient of power series of mean square approximation of data array $(r_i, \Delta T_{avg,i})$.

Residual, nonparaxial part of OPD_{np} corresponds to higher order thermally induced distortions [see Figs. 5(a) and 5(b)] resulting in beam quality degradation.

The surface heat sources [Fig. 5(b)] result in larger OPDs comparing to volume absorption, which agrees well with intuition and engineering practice. The magnitude of near top-hat OPD_{np} [SG_{32} black curves in Figs. 5(a) and 5(b)] is much smaller and has the opposite sign regarding to OPD_{np} calculated for Gaussian beam. Therefore, we can suppose that the proper choice of beam profile can result in near compensation of nonparaxial OPDs at least. It was shown in Figs. 5(a) and 5(b) (green curves) that for SG_5 beam such effect exists, which gives another argument for its beneficial properties in a case of high-power applications. Moreover, having beam shaper transforming $SG_1 \rightarrow SG_5$ and playing with reflecting and refractive elements, we can achieve dynamic compensation of nonparaxial OPDs of all system for variable incident laser power.

To determine the impact of TOEs on laser beam metrics, we have to calculate in first step variance $\sigma = \text{rms}(OPD_{\text{np}})$ taking into account weighting functions corresponding to given beam profile. Furthermore, we calculated Strehl ratio SR_{apr} and M_{apr}^2 parameter applying the following approximated equation:¹

$$SR_{\text{apr}} = \exp[-(2\pi\sigma)^2]; \quad M_{\text{apr}}^2 = \exp[2(\pi\sigma)^2], \quad (13)$$

where $\sigma = \text{rms}(OPD_{\text{np}})$ of nonparaxial OPD_{np} calculated with appropriate weighting function.

The results of calculations for 1-W heat power (10 ppm for 100-kW incident power) were collected in Table 2. The

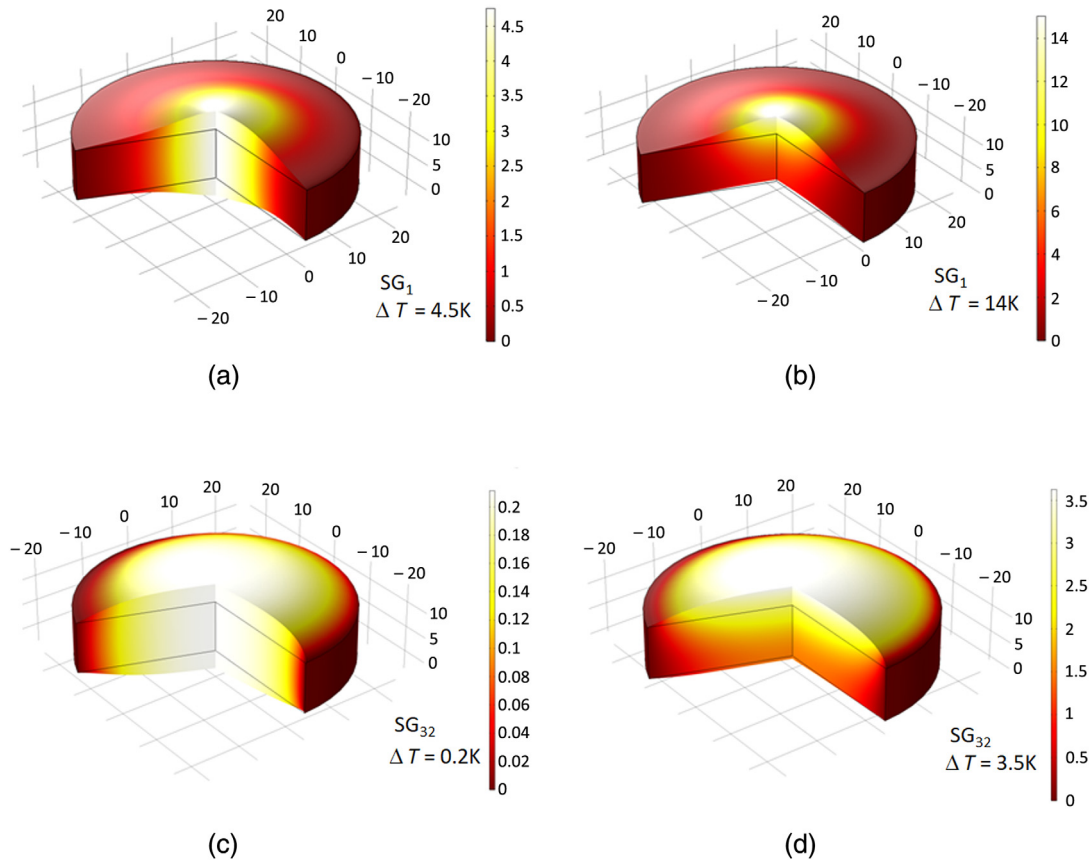


Fig. 4 (a) 3-D map of temperature increase, SG_{1_vol} is the volume absorption for Gaussian beam SG_1 with $2w_1 = 25$ mm, heat power 1 W, $\Delta T = 4.5$ K. (b) 3-D map of temperature increase, SG_{1_surf} is the surface absorption for Gaussian beam SG_1 with $2w_1 = 25$ mm, heat power 1 W, $\Delta T = 14$ K. (c) 3-D map of temperature increase, SG_{32_surf} is the surface absorption for “near top-hat” beam SG_{32} with $2w_{32} = 47$ mm, heat power 1 W, $\Delta T = 0.2$ K. (d) 3-D map of temperature increase, SG_{32_surf} is the surface absorption for near top-hat beam SG_{32} with $2w_1 = 47$ mm, heat power 1 W, $\Delta T = 3.5$ K

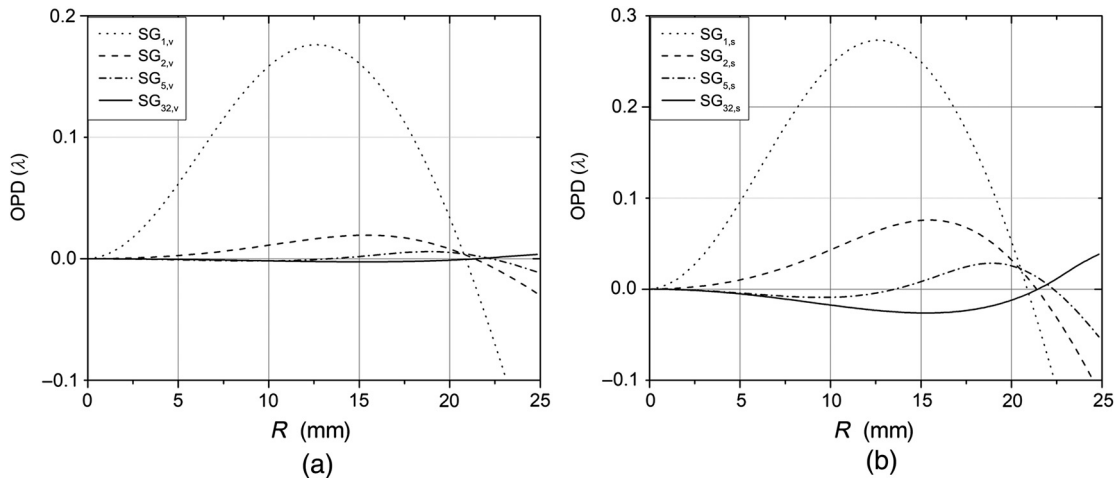


Fig. 5 (a) Nonparaxial OPD_{np} versus radius for four cases of volume heat source, heat power 1 W, SG_1 - dotted, SG_2 - dashed, SG_5 -dash dot, SG_{32} - continuous. (b) Nonparaxial OPD_{np} versus radius for four cases of surface heat source, heat power 1 W, SG_1 - dotted, SG_2 - dashed, SG_5 -dash dot, SG_{32} - continuous.

calculations made for lower power of 0.5 W showed the similar dependencies, only magnitudes have changed proportionally to absorbed power. Thus, we can conclude that the OPDs shown in Figs. 5(a) and 5(b) are typical for

given type of heat source in the framework of linear heat diffusion approximation.

According to theoretical predictions and numerical examples showed here, the values of resulting rms(OPD) and

Table 2 Results of calculations for eight types of heat sources.

Type of source	M_T (1/km)	rms OPD _{np}	M_{apr}^2	SR _{apr}
SG ₁ volume	2.62	0.128	1.378	0.526
SG ₁ surface	4.05	0.198	2.16	0.214
SG ₂ volume	0.59	0.012	1.003	0.994
SG ₂ surface	2.32	0.047	1.045	0.916
SG ₅ volume	0.17	0.0016	1.000	1.000
SG ₅ surface	1.23	0.012	1.003	0.994
SG ₃₂ volume	0.074	0.0017	1.000	1.000
SG ₃₂ surface	0.77	0.017	1.006	0.998

Note: M_T , optical power; rms OPD_{np}, root mean square of nonparaxial OPD_{np}; SR_{apr}, Strehl ratio; M_{apr}^2 , beam quality parameter; $P_{heat} = 1$ W, cylinder sample made of fused silica, $D_{aper} = 50$ mm, and $b = 10$ mm

M_T are proportional to effective absorption or more generally to heat power deposited in the element. Thus, knowing parameter $M_{T,0}$ calculated for given heat power $P_{heat,0}$, we can determine the optical power $M_{T,1}$ for the different heat power $P_{heat,1}$ as follows:

$$M_{T,1} = \kappa_{1,0} M_{T,0}, \quad (14)$$

where $\kappa_{1,0} = P_{heat,1}/P_{heat,0}$ is the ratio of heat powers for cases 0 and 1.

The remaining metrics of optical quality (Strehl ratio SR_{apr} and parameter M_{apr}^2) are highly nonlinear with respect to σ . However, applying the same approach, we can determine the similar relations for SR_{apr,1}, $M_{apr,1}^2$ knowing the parameters SR_{apr,0}, $M_{apr,0}^2$ as follows:

$$M_{apr,1}^2 = (M_{apr,0}^2)^{\kappa_{1,0}^2}; \quad SR_{apr,1} = (SR_{apr,0})^{\kappa_{1,0}^2}. \quad (15)$$

Let us notice that the simplest way to mitigate TOEs is increasing the laser beam size in aperture, e.g., taking collimator of longer focal length and wider aperture. As a rule, lowering power density, the temperature increase basically diminishes.^{10,14} As was shown in Refs. 15 and 16, the average temperature increase is proportional to absorbed power and has nonlinear dependence on laser beam diameter.

An alternative method of TOEs diminishing is application of more flattened than Gaussian laser beam profiles. As shown above, the profile SG₅ should give much lower rms(OPD_{np}) comparing to Gaussian one. On the other hand, the typical beam shaper used to transform SG₁ → SG₅ consists of at least two optical elements (see Refs. 6 and 7) with the first one exposed to Gaussian beam. For complex, multielement optical trains, or multipass systems, e.g., beam cleaners,^{10,11} dynamic mitigation of TOEs of all system can be achieved by application of appropriate beam shaper and playing with mirrors and refractive elements. It is also important for transient, nonstationary regime of operation typical, e.g., laser weapon engagement.

In summary, we have prepared the numerical method to estimate the TOEs for wide class of optical elements valid for

linear heat equation and small absorption approximation. In first step, we have to solve numerically the problem for given type of heat source, absorption efficiency, and sample geometry. The results can be rescaled for different absorptions or heat powers applying Eqs. (14) and (15). The paraxial thermal lensing (determined by M_T) can be compensated by defocusing. The thermo-optic distortions can be transient, time-dependent functions, and for short operation time and relatively low duty, factor can be low as well. The beam quality deteriorates during operation up to the worst case of stationary value typical, e.g., for industry applications. Equations (14) and (15) can be applied also for the estimation of those unstationary, transient effects, knowing additionally time constants of elements. Let us insist on the limits of above approximations. It is valid only for a case of linear, heat equation of constant coefficients, small stresses, and low absorption. Moreover, for higher (comparable with wavelength) variances of OPD, the approximated Eq. (13) is not valid.

4 Conclusions

To achieve the high beam quality and flattened profile in near-field, several beam profiles were analyzed. The SGB SG_p of index $p = 5$ was found as the best compromise.

Furthermore, we have developed the simplified numerical-analytical model of TOEs to estimate acceptable level of heat power dissipated on surfaces and in volumes of optics. Such analysis was performed for several SG_p profiles. In first step, we have to solve problem numerically for given type of heat source, absorption, and sample geometry. The results can be rescaled for different absorption or heat powers applying approximated formulas derived in the paper. The model can be applied also for the estimation of unstationary, transient effects. Moreover, the method of dynamic compensation of TOEs due to application of the appropriate beam profile and combinations of lenses and mirrors was proposed.

Acknowledgments

The work was supported by the National Centre for Research and Development of Poland in the framework of strategic program DOB-1-6/1/PS/2014 and project PBS3/B3/27/2015. We thank Dr. Zbigniew Zawadzki from the Institute of Optoelectronics MUT for critical discussion of the work.

References

1. T. S. Ross, *Laser Beam Quality Metrics*, SPIE Press, Bellingham, Washington (2013).
2. S. De Silvestri et al., "Solid-state laser unstable resonators with tapered reflectivity mirrors: the super-Gaussian approach," *IEEE J. Quantum Electron.* **24**, 1172–1177 (1988).
3. A. Parent, M. Morin, and P. Lavigne, "Propagation of super-Gaussian field distributions," *Opt. Quantum Electron.* **24**, S1071 (1992).
4. V. Bagini et al., "Propagation of axially symmetric flattened Gaussian beams," *J. Opt. Soc. Am. A* **13**, 1385–1393 (1996).
5. M. Santarsiero and R. Borghi, "Correspondence between super-Gaussian and flattened Gaussian beams," *J. Opt. Soc. Am. A* **16**, 188–190 (1999).
6. M. F. Dickey, *Laser Beam Shaping, Theory and Techniques*, CRS Press Taylor & Francis Group, London (2014).
7. J. A. Hoffnagle and C. M. Jefferson, "Design and performance of a refractive optical system that converts a Gaussian to a flattop beam," *Appl. Opt.* **39**, 5488–5499 (2000).
8. "COMSOL multiphysics v. 5.3," <https://www.comsol.com/products>
9. N. Hodgson and H. Weber, *Optical Resonators, Fundamentals, Advanced Concepts and Applications*, Springer, New York (1997).
10. W. Koechner, *Laser Engineering*, Springer, New York (1999).

11. K. L. Dooley et al., "Thermal effects in the input optics of the enhanced laser interferometer gravitational-wave observatory interferometers," *Rev. Sci. Instrum.* **83**, 033109 (2012).
12. C. L. Mueller et al., "The advanced LIGO input optics," *Rev. Sci. Instrum.* **87**, 014502 (2016).
13. L. Pinard et al., "Mirrors used in the LIGO interferometers for first detection of gravitational waves," *Appl. Opt.* **56**, C11–C15 (2017).
14. A. K. Cousins, "Temperature and thermal stress scaling in finite-length end-pumped laser rods," *IEEE J. Quantum Electron.* **28**, 1057–1069 (1992).
15. J. Penano et al., "Optical quality of high-power laser beams in lenses," *J. Opt. Soc. Am. B* **26**(3), 503–510 (2009).
16. B. Fakizi et al., "Laser heating of uncoated optics in a convective medium," *Appl. Opt.* **51**(14), 2573–2580 (2012).

Jan K. Jabczyński is a full professor at Military University of Technology (MUT), Warsaw, Poland. He received his MSc Eng, PhD, and DSc, 1981, 1989, and 1997, respectively. Since 1982, he has been a worker at the Institute of Optoelectronics, MUT. He has been a tutor of applied optics, laser optics, and propagation at MUT. He is the author for about 190 journal papers and conference reports and one handbook. His current research interests include laser optics, coherent optics, high-power laser systems, and diode-pumped lasers.

Mateusz Kaskow received his MSc Eng in electronics from Wrocław University of Technology in 2009 and his PhD in electronics from MUT in 2015. He was with the Institute of Optoelectronics from 2011 to 2017. He is the author for about 40 journal papers and conference

reports. His current research interests include diode-pumped lasers, nonlinear optics, and computer graphics.

Lukasz Gorajek is an assistant professor at MUT. He received his MScEng and PhD degrees in electronics from MUT in 2009 and 2014, respectively. He is with the Institute of Optoelectronics since 2010. He is the author for about 60 journal papers and conference reports. His current research interests include diode-pumped lasers, nonlinear optics, and high-power laser systems.

Krzysztof Kopczyński is an assistant professor at MUT, Warsaw, Poland. He received his MSc Eng and PhD in 1985 and 2000, respectively. Since 1994, he has been with the Institute of Optoelectronics, and for the last eight years, he has worked as a director. He is the author of about 150 journal papers and conference reports and 10 patents. His current research interests include high-power laser systems, laser spectroscopy, lidar systems, diode-pumped lasers, and optoelectronic systems for safety and defense.

Waldemar Zendzian is a full professor at MUT, Warsaw, Poland. He received his MSc Eng degree in technical physics in 1984 and PhD and DSc degrees in electronics in 1993 and 2006, respectively. He is with the Institute of Optoelectronics MUT since 1985. He is the author of about 150 journal papers and conference reports and two handbooks. His current research interests include diode-pumped lasers, nonlinear optics, and quantum electronics.